

**This is a self-archived version of an original article. This version may differ from the original in pagination and typographic details.**

**Author(s):** Matus, María Francisca; Häkkinen, Hannu

**Title:** Atomically Precise Gold Nanoclusters : Towards an Optimal Biocompatible System from a Theoretical–Experimental Strategy

**Year:** 2021

**Version:** Accepted version (Final draft)

**Copyright:** © 2021 Wiley-VCH GmbH

**Rights:** In Copyright

**Rights url:** <http://rightsstatements.org/page/InC/1.0/?language=en>

**Please cite the original version:**

Matus, M. F., & Häkkinen, H. (2021). Atomically Precise Gold Nanoclusters : Towards an Optimal Biocompatible System from a Theoretical–Experimental Strategy. *Small*, 17(27), Article 2005499. <https://doi.org/10.1002/sml.202005499>

1  
2  
3  
4 **Atomically Precise Gold Nanoclusters: Towards an Optimal Biocompatible System**  
5  
6 **from a Theoretical–Experimental Strategy**  
7

8  
9  
10 *María Francisca Matus and Hannu Häkkinen\**  
11

12  
13  
14  
15 Dr. M.F. Matus

16 Department of Physics, Nanoscience Center (NSC)

17 University of Jyväskylä

18 FI-40014 Jyväskylä, Finland  
19  
20  
21

22  
23  
24 Prof. Dr. H. Häkkinen

25 Departments of Physics and Chemistry, Nanoscience Center (NSC)

26 University of Jyväskylä

27 FI-40014 Jyväskylä, Finland  
28  
29

30 E-mail: [hannu.j.hakkinen@jyu.fi](mailto:hannu.j.hakkinen@jyu.fi)  
31  
32  
33  
34  
35  
36

37 **Keywords**  
38

39  
40 Gold Nanoclusters, Biomedical Applications, Nanomedicine, Biocompatibility, Atomistic  
41 Simulations  
42  
43  
44  
45  
46  
47

48  
49 Potential biomedical applications of gold nanoparticles have increasingly been reported with  
50 great promise for diagnosis and therapy of several diseases. However, for such a versatile  
51 nanomaterial, the advantages and potential health risks need to be addressed carefully, as the  
52 available information about their toxicity is limited and inconsistent. Atomically precise gold  
53 nanoclusters (AuNCs) have emerged to overcome this challenge due to their unique features,  
54  
55  
56  
57  
58  
59  
60  
61  
62  
63  
64  
65

1  
2  
3  
4 such as superior stability, excellent biocompatibility, and efficient renal clearance.  
5  
6 Remarkably, the elucidation of their structural and physicochemical properties provided by  
7  
8 theory–experiment investigations offers exciting opportunities for site-specific bio-  
9  
10 functionalization of the nanoparticle surface, which remains a significant concern for most  
11  
12 of the materials in the biomedical field. This Concept highlights the advantages conferred by  
13  
14 atomically precise AuNCs for biomedical applications and the powerful strategy combining  
15  
16 computational and experimental studies towards finding an optimal biocompatible AuNC-  
17  
18 based nanosystem.  
19  
20  
21  
22  
23  
24  
25  
26

## 27 **1. Introduction**

28  
29 Gold nanoparticles (AuNPs) are one of the most exploited nanomaterials in different fields  
30  
31 of science,<sup>[1–3]</sup> attracting special interest in biomedicine.<sup>[4,5]</sup> Over the past decade, diverse  
32  
33 applications of AuNPs have been mainly focused on drug delivery, imaging techniques, and  
34  
35 photothermal therapy.<sup>[6]</sup> Their high versatility has enabled them to show promise in diagnosis  
36  
37 and therapy for several diseases, such as cancers, hepatitis, tuberculosis, and Alzheimer’s  
38  
39 disease.<sup>[7]</sup> However, despite the extensive *in vitro* and *in vivo* studies demonstrating the  
40  
41 efficacy of a large variety of AuNPs, the *in vivo* toxicity remains a significant problem,  
42  
43 directly related to their size and aggregation.<sup>[8,9]</sup> Either their large size (typically above 50  
44  
45 nm) or the eventual formation of large aggregates (around 20–100 nm) means that the AuNPs  
46  
47 cannot be metabolized<sup>[10]</sup> and are unable to escape the reticuloendothelial system (RES), with  
48  
49 the consequent accumulation in some organs, like liver and spleen.<sup>[7]</sup> Therefore, with the  
50  
51 increasing progress of bio-applications, it becomes critical to evaluate the toxicity and  
52  
53 biocompatibility, which particularly in the case of AuNPs, is still contradictory.<sup>[3]</sup>  
54  
55  
56  
57  
58  
59  
60  
61  
62  
63  
64  
65

1  
2  
3  
4  
5  
6  
7 In the past 10+ years, a singular type of ultra-small AuNPs, so-called gold nanoclusters  
8 (AuNCs), has emerged.<sup>[11,12]</sup> Unlike colloidal and polydisperse gold nanoparticles, AuNCs  
9  
10 are composed of a few to some hundreds of gold atoms, which corresponds to NPs smaller  
11  
12 than 2 nm metal core diameter with a uniform crystal structure. AuNCs are unique since their  
13  
14 structures can be determined to atomic precision by using single crystal X-ray diffraction  
15  
16 methods.<sup>[11,13,14]</sup> This fact has enabled accurate studies of their physicochemical properties,  
17  
18 highlighting their atomically precise structure that can bring much more control for binding  
19  
20 selectivity, offering a higher precision in the exploration of their potential applications, than  
21  
22 what can be achieved with the colloidal noble metal NPs. In biomedicine, they have gained  
23  
24 growing interest due to their extraordinary properties such as facile synthesis, superior  
25  
26 stability, excellent biocompatibility and efficient renal clearance.<sup>[14,15]</sup>  
27  
28  
29  
30  
31  
32  
33  
34  
35  
36  
37

38 Functionalization of their surface takes the AuNCs to the next level allowing them to exert  
39  
40 their action at a specific site. However, it also creates one of the main challenges because the  
41  
42 chemical and physical properties of AuNCs can be significantly affected by their surface  
43  
44 modification.<sup>[16]</sup> Functionalization also increases the system's complexity due to the high  
45  
46 number of atomic and molecular interactions involved, which, together with its small size,  
47  
48 hinder its development at the experimental level. This is where the use of computational  
49  
50 modeling begins to become particularly important. Computational tools provide useful  
51  
52 approaches to addressing several challenges in the design of nanosystems, including the need  
53  
54 for a better understanding of nanoparticle behavior and the prediction of different  
55  
56 physicochemical properties at the atomic level. The advances in the field of thiolate-protected  
57  
58  
59  
60  
61  
62  
63  
64  
65

1  
2  
3  
4 AuNCs have been powered by this close interaction of experimental and theoretical studies.  
5  
6 To date, several precise structures have been revealed either by X-ray diffraction or  
7  
8 theoretically predicted by employing density functional theory (DFT) computation.<sup>[17]</sup>  
9  
10 Combination of theory and experiment has permitted the elucidation of several properties,  
11  
12 including electronic structures, luminescence, optical absorption, as well as the structural  
13  
14 patterns of their high symmetric cores and their protecting ligand motifs.<sup>[17,18]</sup> This well-  
15  
16 defined structural information offers a particularly attractive chance for a better  
17  
18 understanding of the structure–property relationships of these intriguing systems and the  
19  
20 unique opportunity for highly-controlled adjustments of specific features in order to increase  
21  
22 the desired properties in different applications.  
23  
24  
25  
26  
27  
28  
29  
30  
31

32 This Concept focuses specifically on the advantages conferred by atomically precise AuNCs  
33  
34 for biomedical applications and the powerful strategic approach of using theory and  
35  
36 experiment in a complementary manner towards finding an optimal biocompatible AuNC-  
37  
38 based nanosystem.  
39  
40  
41  
42  
43  
44

## 45 **2. The Unique Properties of Ultra-small AuNCs for Biomedical Applications**

46  
47  
48 Potential biomedical applications of any nanosystem are mainly linked to some critical  
49  
50 factors, such as size, physicochemical properties and surface chemistry.<sup>[19]</sup> AuNCs possess a  
51  
52 unique combination of these features, which makes them particularly promising in the field  
53  
54 of biomedicine. Their ultra-small size favors the renal clearance<sup>[20,21]</sup> and helps them evade  
55  
56 the uptake by the RES.<sup>[22]</sup> Likewise, their small size and the benefit from the enhanced  
57  
58  
59  
60  
61  
62  
63  
64  
65

1  
2  
3  
4 permeability and retention (EPR)<sup>[23]</sup> and nanomaterials-induced endothelial cell leakiness  
5  
6 (NanoEL)<sup>[24]</sup> effects allow exceptional tumor accumulation properties.  
7  
8  
9

10  
11 Highly stable optical properties are another advantage. AuNCs display molecular-like  
12  
13 properties such as discrete electronic transitions, leading to photoluminescence (PL)  
14  
15 properties tunable from the ultra-violet (UV) to near-infrared (NIR) region,<sup>[25,26]</sup> which offers  
16  
17 great potential for their detection *in vivo* by multimodal imaging techniques with excellent  
18  
19 performance, overcoming difficulties related to PL quenching of larger plasmonic AuNPs.<sup>[15]</sup>  
20  
21  
22  
23  
24  
25  
26  
27

28  
29 Proper surface functionalization is also critical for the biocompatibility of the nanosystem.  
30  
31 The surface ligands significantly influence the solubility, stability, and determine the  
32  
33 interactions of the nanomaterial with the environment.<sup>[27]</sup> The biocompatibility of the AuNCs  
34  
35 can be further improved by taking advantage of their facile surface modification. Several  
36  
37 efficient strategies have been developed to synthesize AuNCs protected by thiolate ligands  
38  
39 with atomic precision,<sup>[14]</sup> resulting in water-soluble AuNCs, which are especially desired in  
40  
41 applications for biological systems. Atomically precise AuNCs functionalized with other  
42  
43 biocompatible molecules offer unique opportunities in theranostics, allowing more control  
44  
45 over such sensitive and challenging issues as protein corona formation, *in vivo*  
46  
47 biodistribution, and cellular uptake efficiency, to name a few.<sup>[28]</sup> Considering this huge  
48  
49 potential within the field of nanomedicine, investigations using atomically precise, water-  
50  
51 soluble, and monodisperse AuNCs, need to be emphasized.  
52  
53  
54  
55  
56  
57  
58  
59  
60  
61  
62  
63  
64  
65

1  
2  
3  
4 In radiotherapy, which is one of the leading types of cancer treatment, AuNCs with  
5  
6 atomically precise structure provide a remarkable opportunity for radiosensitizer  
7  
8 investigations (Figure 1). Beyond just showing enhancement of the radiotherapeutic activity,  
9  
10 they allow to accurately associate radiosensitizer properties with the inner core structure and  
11  
12 ligands.<sup>[29]</sup> For instance, Xie group (2014 and 2015) has developed and studied *in vivo* a  
13  
14 series of sub-2 nm glutathione (GSH)-protected AuNCs with these features, such as Au<sub>10-</sub>  
15  
16 <sub>12</sub>(GSH)<sub>10-12</sub>,<sup>[30]</sup> Au<sub>25</sub>(GSH)<sub>18</sub>,<sup>[31]</sup> and Au<sub>29-43</sub>(GSH)<sub>27-37</sub><sup>[32]</sup> NCs, which showed a ultrahigh  
17  
18 tumor uptake and low toxicity. They found that the AuNCs could readily escape from the  
19  
20 RES and accumulate in tumors *via* the improved EPR effect, leading to enhanced cancer  
21  
22 radiotherapy. In 2019, Jia and coworkers reported a structurally defined  
23  
24 alkynyl(levonorgestrel)-protected Au<sub>8</sub> NC as an effective and biocompatible radiosensitizer  
25  
26 that causes irreversible apoptosis of tumor cells due to their localized production of reactive  
27  
28 oxygen species (ROS).<sup>[29]</sup> *In vivo* models showed a significant inhibition rate of 74.2 % when  
29  
30 tumors are treated with Au<sub>8</sub>(levonorgestrel)<sub>8</sub> NCs and an X-ray dose of 4 Gray (Gy)  
31  
32 compared to tumors irradiated with X-ray alone. Recently, targeting capacity of  
33  
34 radiosensitizers for prostate cancer cells has also been reported with promising results. Luo  
35  
36 *et al.* (2019) designed Au<sub>25</sub> NCs protected with a peptide-tagged prostate specific membrane  
37  
38 antigen targeting ligand (CY-PSMA-1) with the ability to target PSMA receptor positive  
39  
40 cancer cells (PC3pip).<sup>[33]</sup> The results demonstrated a significantly enhanced tumor-  
41  
42 suppressing efficacy of the Au<sub>25</sub>S<sub>(18-m)</sub>(CY-PSMA-1)<sub>m</sub> (m=0–18) NCs *in vivo* when combined  
43  
44 with X-ray irradiation (6 Gy) and showed fast renal clearance from the mice body.  
45  
46  
47  
48  
49  
50  
51  
52  
53  
54  
55  
56

57 Targeting strategies in AuNCs with atomic precise structures has expanded well beyond the  
58  
59 cancer nanomedicine field. For example, by replacing GSH ligands with (4-  
60  
61  
62  
63  
64  
65

1  
2  
3  
4 mercaptobutyl)triphenyl-phosphonium bromide (MTPB) on fluorescent Au<sub>18</sub>(GSH)<sub>14</sub> NCs  
5  
6 through a ligand exchange method, mitochondrial targeting was achieved.<sup>[34]</sup> While the  
7  
8 unmodified Au<sub>18</sub>(GSH)<sub>14</sub> preferably accumulated in lysosomes, the resulting water-soluble  
9  
10 Au<sub>18</sub>(GSH)<sub>12</sub>(MTPB)<sub>2</sub> NCs showed higher accumulation at the mitochondrial site with their  
11  
12 initial optical properties largely unaffected. Due to the central role of mitochondria in critical  
13  
14 cellular processes such as metabolism and apoptosis, this approach is highly attractive to  
15  
16 stimulate extensive studies and potential applications for diagnosis and treatment of several  
17  
18 diseases, such as diabetes, obesity, neurodegenerative diseases, and cancers<sup>[35]</sup> at the cell and  
19  
20 organelle levels.  
21  
22  
23  
24  
25  
26  
27  
28  
29  
30

31 Another growing global threat is antibiotic resistance.<sup>[36]</sup> Thus, alternatives to conventional  
32  
33 antibiotics that address bacterial infections are highly desirable. For several years, the NP  
34  
35 activity against multidrug-resistant pathogens has been demonstrated.<sup>[37,38]</sup> However,  
36  
37 potential antimicrobial activity of AuNPs reduced to the NC range remained practically  
38  
39 unexplored until 2017 when Zheng and colleagues studied the antibacterial potential of 6-  
40  
41 mercaptohexanoic acid (MHA)-protected Au<sub>25</sub> NCs on both Gram-positive and Gram-  
42  
43 negative strains.<sup>[39]</sup> Au<sub>25</sub>(MHA)<sub>18</sub> NCs showed a high wide-spectrum antimicrobial activity,  
44  
45 killing more than 90 % of Gram-positive (*Staphylococcus aureus*, *Staphylococcus epidermis*,  
46  
47 and *Bacillus subtilis*) and Gram-negative bacteria (*Escherichia coli* and *Pseudomonas*  
48  
49 *aeruginosa*) with a dose of 0.1 mM. They found that Au<sub>25</sub>(MHA)<sub>18</sub> NCs could induce a  
50  
51 metabolic imbalance in the cells, leading to a significant increase of intracellular ROS  
52  
53 production, which confers the bacteria-killing effect. In sharp contrast, the observed  
54  
55 antimicrobial effect is absent in the AuNPs counterparts protected with the same ligand. This  
56  
57  
58  
59  
60  
61  
62  
63  
64  
65



1  
2  
3  
4 study provides a proof of principle for the utilization of AuNCs as an alternative wide-  
5  
6 spectrum antimicrobial agent and, at the same time, with potential high biocompatibility in  
7  
8 the host human cells due to the noble qualities of gold<sup>[40,41]</sup> (Figure 1). Even more interesting,  
9  
10 AuNCs possess higher structural stability than silver (Ag) NPs and AgNCs,<sup>[42]</sup> which have  
11  
12 led the investigations in this field due to the intrinsic antimicrobial capacity of Ag.<sup>[43]</sup> Hence,  
13  
14 AuNCs could be one of the best candidates for the development of a new generation of  
15  
16 antimicrobial agents.  
17  
18  
19  
20  
21  
22

23  
24 The outstanding role of atomistically well-defined monodisperse AuNCs as contrast agents  
25  
26 in biological imaging applications has also been demonstrated through site-specific  
27  
28 conjugation to biomolecules<sup>[44,45]</sup> (Figure 1). AuNCs would allow addressing some  
29  
30 fundamental challenges in this field, such as the long-term stability of markers and their  
31  
32 biocompatibility for clinical applications,<sup>[46]</sup> offering distinctive features to the development  
33  
34 of more direct and robust tracking strategies *in vitro* and *in vivo*. In 2014, Marjomäki *et al.*  
35  
36 reported a site-specific covalent conjugation of water-soluble *para*-mercaptobenzoic acid  
37  
38 (*p*MBA)-protected Au<sub>102</sub> NCs, functionalized by a thiol-reactive linker (*N*-(6-  
39  
40 hydroxyhexyl)maleimide) to target cysteine sites of capsid proteins in echovirus 1 (EV1) and  
41  
42 Coxsackievirus B3 (CVB3) without compromising their infectivity.<sup>[44]</sup> The well-defined  
43  
44 structures of both maleimide functionalized-Au<sub>102</sub>(*p*MBA)<sub>44</sub> NCs and viruses capsid allowed  
45  
46 analyzing the specific spatial ordering of enterovirus–cluster conjugates in both virus types  
47  
48 through transmission electron microscopy (TEM). One year later and taking advantage of  
49  
50 this strategy, Au<sub>102</sub>(*p*MBA)<sub>44</sub> NCs were utilized for noncovalent linking to the capsid of EV1  
51  
52 and CVA9 enteroviruses.<sup>[45]</sup> AuNCs were conjugated to a Pleconaril drug-like molecule,  
53  
54 which was used to target site-specifically the hydrophobic pocket of the virus capsid,  
55  
56  
57  
58  
59  
60  
61  
62  
63  
64  
65

1  
2  
3  
4 enabling the visualization of the viruses *via* TEM while retaining their infectivity. These  
5  
6 approaches may be extended not only for structural studies of viral uncoating, but also for  
7  
8 revealing more fundamentals of virus and other biomolecules entry pathways into cells. In  
9  
10 this context, a AuNC-labeled fibroblast growth factor 21 (FGF21) tracking technique was  
11  
12 reported in human primary adipocytes.<sup>[47]</sup> By using *meta*-mercaptobenzoic acid (3MBA)-  
13  
14 protected Au<sub>144</sub> NCs conjugated with FGF21 and cryo-electron tomography (cryo-ET),  
15  
16 Azubel and coworkers (2019) were able to capture different states of activation,  
17  
18 internalization, and traffic of the FGF21/FGFR1c/β-Klotho (FGF-receptor-cofactor)  
19  
20 complex demonstrating its clathrin-dependent pathway endocytosis.<sup>[47]</sup> The paired or  
21  
22 unpaired FGF21 functionalized-Au<sub>144</sub>(3MBA)<sub>-40</sub> NCs distribution in different vesicular  
23  
24 compartments helped to confirm the overall 2:2:2 stoichiometry of the ternary complex in  
25  
26 the human fat cells and observe its disruption at specific levels in the pathway. This is the  
27  
28 first study in which, through Au<sub>144</sub>(3MBA)<sub>-40</sub> NCs labeling, a three-dimensional picture of  
29  
30 the entire endocytosis pathway is achieved.

31  
32  
33 The photoluminescence of AuNCs is another significant feature that makes them a promising  
34  
35 agent for biological imaging and medical diagnosis.<sup>[48]</sup> In a recent study, Liu *et al.* (2019)  
36  
37 demonstrated the potential of water-soluble Au<sub>25</sub>(GSH)<sub>18</sub> NCs as an efficient near-infrared II  
38  
39 (NIR-II) fluorophore in *in vivo* models.<sup>[49]</sup> Au<sub>25</sub>(GSH)<sub>18</sub> NCs can emit fluorescence at 1100–  
40  
41 1350 nm and showed unique features of particular relevance for biological and clinical  
42  
43 applications, such as high quantum yield (QY) that can be further increased by metal-atom  
44  
45 doping, and efficient renal clearance even at an ultrahigh dose of 100 mg kg<sup>-1</sup>. It is noteworthy  
46  
47 that most of the nanomaterials (inorganic and organic) that have shown promising features  
48  
49 as agents for bioimaging meet only one of these requirements.<sup>[49]</sup> Thus, it is time to expand  
50  
51 the investigations of AuNCs-based agents in this field, but now including comparisons with  
52  
53  
54  
55  
56  
57  
58  
59  
60  
61  
62  
63  
64  
65

1  
2  
3  
4 more promising and emerging nanostructures, such as palladium (Pd)-based  
5  
6 nanomaterials.<sup>[50]</sup> Interestingly, Pd nanosheets (16 nm) were reported to have high  
7  
8 photothermal efficiency and showed superior stability, measured against AuNPs  
9  
10 (nanorods).<sup>[51]</sup> However, these findings might substantively differ when the point of  
11  
12 comparison is AuNCs instead, due to their exceptional features described above, which can  
13  
14 only be obtained when the size of NPs is reduced to the NC range.  
15  
16  
17  
18  
19  
20  
21  
22

### 23 **3. Manipulation of the System at Atomic Level: In Pursuit of the Most Realistic** 24 25 **Theoretical Model** 26

27  
28  
29 Clearly, the extraordinary properties that atomically precise AuNCs have exhibited in  
30  
31 experimental research, place them as one of the most promising nanomaterials within the  
32  
33 field of biomedicine. However, in order to extend their applications and achieve their clinical  
34  
35 translation, some current fundamental challenges need to be considered and understood in  
36  
37 more detail, such as improving the PL quantum yield, increasing the yield of the synthesis,  
38  
39 and precisely controlling the surface modification.<sup>[16]</sup> To achieve this purpose, an  
40  
41 interdisciplinary strategy becomes critical. The use of theoretical models either as a  
42  
43 predictive tool or as complementary to experimental work could provide crucial information  
44  
45 for the design of optimal AuNC-based biocompatible systems, including their geometric  
46  
47 structure, electronic structure, reaction mechanisms, structure–activity relationship as well as  
48  
49 the effects of the surrounding environment (**Figure 2**).  
50  
51  
52  
53  
54  
55  
56  
57  
58  
59  
60  
61  
62  
63  
64  
65

1  
2  
3  
4 DFT calculations have been extensively used and synergistically combined with experiments  
5  
6 for AuNCs characterization, showing an outstanding performance in their structure and  
7  
8 properties elucidation.<sup>[52]</sup> By this method, some aspects like general structures, core-shell  
9  
10 geometries, and isomerization mechanisms of diverse atomically precise AuNCs have been  
11  
12 predicted with high accuracy.<sup>[17,53,54]</sup> Furthermore, DFT has supported the development of a  
13  
14 molecular mechanics force field for thiolate-protected AuNCs compatible with the well-  
15  
16 known biomolecular force field AMBER.<sup>[55]</sup> This allows investigating the dynamics of the  
17  
18 AuNCs in a more realistic biological environment (i.e., including solvent, counterions) by  
19  
20 employing classical molecular dynamics (MD) simulations. Combined with the existing  
21  
22 biomolecular force fields in AMBER, interactions between the gold clusters and  
23  
24 biomolecules, such as proteins, cell membranes, or nucleic acids can be explored in long time  
25  
26 scales (in principle, from hundreds of nanoseconds to microsecond by using supercomputers)  
27  
28 with an all-atom description. The precise atomic structure of AuNCs is crucial in the  
29  
30 construction of these theoretical models and particularly relevant for investigations of the  
31  
32 bio-nano interface and addressing the challenge of protein corona formation in an exhaustive  
33  
34 way. Correlation of these theoretical predictions with experimental data from methods like  
35  
36 X-ray diffraction and Ultraviolet-visible (UV-vis) spectroscopy offers the possibility to  
37  
38 determine which features of the AuNC can be adapted to increase the desired properties.  
39  
40  
41  
42  
43  
44  
45  
46  
47  
48  
49  
50

51 Thiolate-for-thiolate ligand exchange reaction is a well-established technique and widely  
52  
53 used for surface modification of monolayer-protected AuNCs.<sup>[56-58]</sup> Although this strategy  
54  
55 had been utilized for many years since its origin, it was not until 2012 when Heinecke and  
56  
57 colleagues reported the structural basis of this strategy by employing a computational-  
58  
59  
60  
61  
62  
63  
64  
65

1  
2  
3  
4 experimental approach.<sup>[59]</sup> They used *p*-bromobenzene thiol (*p*BBT) as the incoming ligand  
5  
6 and performed the exchange reaction to obtain the first single-crystal X-ray structure of a  
7  
8 partially exchanged  $\text{Au}_{102}(\text{pMBA})_{40}(\text{pBBT})_4 \text{ NC}$ . They studied the regioselectivity of the  
9  
10 reaction based on the 22 symmetry-unique *p*MBA ligand sites of  $\text{Au}_{102}(\text{pMBA})_{44}$  and  
11  
12 postulated the mechanistic pathway for the reaction by DFT calculations. Ligand place-  
13  
14 exchange was exhibited in 2 of the 22 symmetrically unique ligand sites, each of them bonded  
15  
16 to a different solvent-exposed gold atom. Together with a complete reaction path modeling  
17  
18 both thiol and thiolate incoming ligands by DFT, the authors suggested an associative  
19  
20 exchange mechanism. Following the same line, Rojas-Cervellera *et al.* (2017) studied the  
21  
22 molecular mechanism of ligand exchange reaction involving AuNCs and proteins by  
23  
24 combining classical and *ab initio* quantum mechanics/molecular mechanics (QM/MM) MD  
25  
26 simulations.<sup>[60]</sup> Inspired by the experimental work of Ackerson group (2006), they modeled  
27  
28 the conjugation of  $\text{Au}_{25}(\text{GSH})_{18}^- \text{ NC}$  with a single chain Fv (scFv) fragment of the NC10  
29  
30 antibody in water in order to obtain an atomistic description of this reaction.<sup>[61]</sup> Two  
31  
32 particular sites in the  $\text{Au}_{25}$  V-shaped staple were considered (side thiolate and apex thiolate)  
33  
34 and thus, two different routes were explored to determine which one is more readily  
35  
36 exchanged. Calculations showed that the reaction follows an associative  $\text{S}_{\text{N}}2$ -like reaction  
37  
38 mechanism and the substitution of the side ligand is favored over the apex one, which  
39  
40 interestingly, is in high accordance with the study described above using  
41  
42  $\text{Au}_{102}(\text{pMBA})_{40}(\text{pBBT})_4 \text{ NCs}$ .<sup>[59]</sup> The results also suggested that the presence of positively  
43  
44 charged residues surrounding the incoming ligand facilitates the adsorption of the protein on  
45  
46 the AuNC surface. These approaches are attractive for site-selective modification of AuNCs  
47  
48 displaying desired properties for stable and functional AuNC-biomolecule conjugates.  
49  
50  
51  
52  
53  
54  
55  
56  
57  
58  
59  
60  
61  
62  
63  
64  
65

1  
2  
3  
4 In 2016, Salorinne *et al.* reported a complete  $^1\text{H}$  and  $^{13}\text{C}$  nuclear magnetic resonance (NMR)  
5  
6 chemical shifts assignment for all ligands of the atomically precise  $\text{Au}_{102}(\text{pMBA})_{44}$  NC in  
7  
8 water by employing a combination of multidimensional NMR methods, DFT calculations,  
9  
10 and MD simulations.<sup>[62]</sup> By using these computational techniques, it was possible to obtain a  
11  
12 precise structural and dynamical information of the ligand shell and correlate it with ligand  
13  
14 symmetry environments observed in the single-crystal X-ray structure.<sup>[63]</sup> This study is  
15  
16 particularly attractive for accurate functionalization strategies and gives the potential to  
17  
18 control and understand in more detail the bio–nano interface and the transformations that  
19  
20 AuNCs undergo in the biological environment.  
21  
22  
23  
24  
25  
26  
27  
28

29 Another interdisciplinary study was carried out in 2017, where the atomic structure and  
30  
31 dynamics of the ligand layer of  $\text{Au}_{68}(\text{3MBA})_{\sim 32}$  and  $\text{Au}_{144}(\text{3MBA})_{\sim 40}$  NCs was revealed.<sup>[64]</sup>  
32  
33 By a combination of MD simulations and DFT calculations, and supported by NMR, UV-vis  
34  
35 absorption, and Infrared (IR) spectroscopy the authors suggested a distinct chemistry in the  
36  
37 ligand–metal interface, which is absent in other known thiol-stabilized AuNCs. Interestingly,  
38  
39 they found weak  $\pi$ –Au and  $\text{O}=\text{C}-\text{OH}\cdots\text{Au}$  interactions protecting the metal core in addition  
40  
41 to the covalent S–Au bond formation. This finding could support some particular features  
42  
43 observed previously in 3MBA-protected AuNCs, such as their reactivity to thiol-modified  
44  
45 DNA and proteins<sup>[65]</sup> and the unusually low ligand coverage in the  $\text{Au}_{144}(\text{3MBA})_{\sim 40}$  NC.<sup>[66]</sup>  
46  
47  
48  
49 In addition to explaining or validating experimental evidence, this finding offers new  
50  
51 possibilities for the development of novel hybrid nanosystems based on 3MBA-protected  
52  
53 AuNCs (e.g., as drug delivery systems, biosensors) and understand their functionalization  
54  
55  
56  
57  
58  
59  
60  
61  
62  
63  
64  
65  
66  
67  
68  
69  
70  
71  
72  
73  
74  
75  
76  
77  
78  
79  
80  
81  
82  
83  
84  
85  
86  
87  
88  
89  
90  
91  
92  
93  
94  
95  
96  
97  
98  
99  
100  
101  
102  
103  
104  
105  
106  
107  
108  
109  
110  
111  
112  
113  
114  
115  
116  
117  
118  
119  
120  
121  
122  
123  
124  
125  
126  
127  
128  
129  
130  
131  
132  
133  
134  
135  
136  
137  
138  
139  
140  
141  
142  
143  
144  
145  
146  
147  
148  
149  
150  
151  
152  
153  
154  
155  
156  
157  
158  
159  
160  
161  
162  
163  
164  
165  
166  
167  
168  
169  
170  
171  
172  
173  
174  
175  
176  
177  
178  
179  
180  
181  
182  
183  
184  
185  
186  
187  
188  
189  
190  
191  
192  
193  
194  
195  
196  
197  
198  
199  
200  
201  
202  
203  
204  
205  
206  
207  
208  
209  
210  
211  
212  
213  
214  
215  
216  
217  
218  
219  
220  
221  
222  
223  
224  
225  
226  
227  
228  
229  
230  
231  
232  
233  
234  
235  
236  
237  
238  
239  
240  
241  
242  
243  
244  
245  
246  
247  
248  
249  
250  
251  
252  
253  
254  
255  
256  
257  
258  
259  
260  
261  
262  
263  
264  
265  
266  
267  
268  
269  
270  
271  
272  
273  
274  
275  
276  
277  
278  
279  
280  
281  
282  
283  
284  
285  
286  
287  
288  
289  
290  
291  
292  
293  
294  
295  
296  
297  
298  
299  
300  
301  
302  
303  
304  
305  
306  
307  
308  
309  
310  
311  
312  
313  
314  
315  
316  
317  
318  
319  
320  
321  
322  
323  
324  
325  
326  
327  
328  
329  
330  
331  
332  
333  
334  
335  
336  
337  
338  
339  
340  
341  
342  
343  
344  
345  
346  
347  
348  
349  
350  
351  
352  
353  
354  
355  
356  
357  
358  
359  
360  
361  
362  
363  
364  
365  
366  
367  
368  
369  
370  
371  
372  
373  
374  
375  
376  
377  
378  
379  
380  
381  
382  
383  
384  
385  
386  
387  
388  
389  
390  
391  
392  
393  
394  
395  
396  
397  
398  
399  
400  
401  
402  
403  
404  
405  
406  
407  
408  
409  
410  
411  
412  
413  
414  
415  
416  
417  
418  
419  
420  
421  
422  
423  
424  
425  
426  
427  
428  
429  
430  
431  
432  
433  
434  
435  
436  
437  
438  
439  
440  
441  
442  
443  
444  
445  
446  
447  
448  
449  
450  
451  
452  
453  
454  
455  
456  
457  
458  
459  
460  
461  
462  
463  
464  
465  
466  
467  
468  
469  
470  
471  
472  
473  
474  
475  
476  
477  
478  
479  
480  
481  
482  
483  
484  
485  
486  
487  
488  
489  
490  
491  
492  
493  
494  
495  
496  
497  
498  
499  
500  
501  
502  
503  
504  
505  
506  
507  
508  
509  
510  
511  
512  
513  
514  
515  
516  
517  
518  
519  
520  
521  
522  
523  
524  
525  
526  
527  
528  
529  
530  
531  
532  
533  
534  
535  
536  
537  
538  
539  
540  
541  
542  
543  
544  
545  
546  
547  
548  
549  
550  
551  
552  
553  
554  
555  
556  
557  
558  
559  
560  
561  
562  
563  
564  
565  
566  
567  
568  
569  
570  
571  
572  
573  
574  
575  
576  
577  
578  
579  
580  
581  
582  
583  
584  
585  
586  
587  
588  
589  
590  
591  
592  
593  
594  
595  
596  
597  
598  
599  
600  
601  
602  
603  
604  
605  
606  
607  
608  
609  
610  
611  
612  
613  
614  
615  
616  
617  
618  
619  
620  
621  
622  
623  
624  
625  
626  
627  
628  
629  
630  
631  
632  
633  
634  
635  
636  
637  
638  
639  
640  
641  
642  
643  
644  
645  
646  
647  
648  
649  
650  
651  
652  
653  
654  
655  
656  
657  
658  
659  
660  
661  
662  
663  
664  
665  
666  
667  
668  
669  
670  
671  
672  
673  
674  
675  
676  
677  
678  
679  
680  
681  
682  
683  
684  
685  
686  
687  
688  
689  
690  
691  
692  
693  
694  
695  
696  
697  
698  
699  
700  
701  
702  
703  
704  
705  
706  
707  
708  
709  
710  
711  
712  
713  
714  
715  
716  
717  
718  
719  
720  
721  
722  
723  
724  
725  
726  
727  
728  
729  
730  
731  
732  
733  
734  
735  
736  
737  
738  
739  
740  
741  
742  
743  
744  
745  
746  
747  
748  
749  
750  
751  
752  
753  
754  
755  
756  
757  
758  
759  
760  
761  
762  
763  
764  
765  
766  
767  
768  
769  
770  
771  
772  
773  
774  
775  
776  
777  
778  
779  
780  
781  
782  
783  
784  
785  
786  
787  
788  
789  
790  
791  
792  
793  
794  
795  
796  
797  
798  
799  
800  
801  
802  
803  
804  
805  
806  
807  
808  
809  
810  
811  
812  
813  
814  
815  
816  
817  
818  
819  
820  
821  
822  
823  
824  
825  
826  
827  
828  
829  
830  
831  
832  
833  
834  
835  
836  
837  
838  
839  
840  
841  
842  
843  
844  
845  
846  
847  
848  
849  
850  
851  
852  
853  
854  
855  
856  
857  
858  
859  
860  
861  
862  
863  
864  
865  
866  
867  
868  
869  
870  
871  
872  
873  
874  
875  
876  
877  
878  
879  
880  
881  
882  
883  
884  
885  
886  
887  
888  
889  
890  
891  
892  
893  
894  
895  
896  
897  
898  
899  
900  
901  
902  
903  
904  
905  
906  
907  
908  
909  
910  
911  
912  
913  
914  
915  
916  
917  
918  
919  
920  
921  
922  
923  
924  
925  
926  
927  
928  
929  
930  
931  
932  
933  
934  
935  
936  
937  
938  
939  
940  
941  
942  
943  
944  
945  
946  
947  
948  
949  
950  
951  
952  
953  
954  
955  
956  
957  
958  
959  
960  
961  
962  
963  
964  
965  
966  
967  
968  
969  
970  
971  
972  
973  
974  
975  
976  
977  
978  
979  
980  
981  
982  
983  
984  
985  
986  
987  
988  
989  
990  
991  
992  
993  
994  
995  
996  
997  
998  
999  
1000

1  
2  
3  
4  
5  
6  
7 Motivated by the ability of AuNCs as biocompatible contrast agents in virus imaging  
8 demonstrated experimentally and described in the previous section,<sup>[45]</sup> Pohjolainen and  
9 coworkers (2017) performed a series of all-atom MD simulations combined with non-  
10 equilibrium free energy calculations to study in detail the effect of  $\text{Au}_{102}(\text{pMBA})_{44}$  NCs on  
11 the binding affinity of the AuNC-linked pocket factor–virus complex.<sup>[67]</sup> Half- and fully  
12 deprotonated states of *p*MBA ligand layer were considered and included in a complete system  
13 containing the full EV1 virus and the hydrophobic pocket factors in water, making it able to  
14 obtain molecule-scale structural information and complement the experimental findings.  
15 They found that the binding affinity of AuNC-linked pocket factor–virus is pH-sensitive.  
16 Specifically, the affinity of this complex (before AuNC labeling) is unaffected when fully  
17 deprotonated  $\text{Au}_{102}(\text{pMBA})_{44}$  NCs are conjugated to the pocket factor, whereas the half  
18 deprotonated state induces a higher binding affinity, but more importantly, in none of two  
19 conditions a decrease in the affinity is observed. This theoretical approach exhibited results  
20 that agree qualitatively with the experiments<sup>[45]</sup> and represents a useful methodology that,  
21 combined with tools for drug design like virtual screening, could be used for designing new  
22 biomarkers and optimal strategies for virus-imaging applications.  
23  
24  
25  
26  
27  
28  
29  
30  
31  
32  
33  
34  
35  
36  
37  
38  
39  
40  
41  
42  
43  
44  
45  
46  
47

#### 48 **4. Conclusion and Future Perspectives**

49  
50 It is clear that atomically precise AuNCs have helped to revolutionize the field of  
51 nanomedicine due to their good biocompatibility and extraordinary physicochemical  
52 properties. Although the development of AuNCs-based strategies is still in its infancy, their  
53 optical features together with low toxicity demonstrated in varied applications, make them  
54  
55  
56  
57  
58  
59  
60  
61  
62  
63  
64  
65

1  
2  
3  
4 promising to overcome challenges like biostability and cytotoxicity that remain pending for  
5  
6 most of the nanomaterials. Notably, the increasingly detailed knowledge of the structural and  
7  
8 physicochemical properties provided by the close connection between theoretical and  
9  
10 experimental studies, offers exciting opportunities for site-specific bio-functionalization of  
11  
12 the nanoparticle surface. Understanding the details of the internal structure and stability of  
13  
14 the ligand shell at atomic level, which is particularly well-defined in these systems, allows  
15  
16 accurate control of the potential surface functional groups. Thus, their precise atomic  
17  
18 structure provides remarkable advantages for potential applications in drug delivery,  
19  
20 biomolecule labelling and targeting. Recent advances in force fields will allow exploration  
21  
22 of the interaction of the engineered AuNCs with the desired environment *via* atomistic  
23  
24 simulations as well as gaining more insight on the nano–bio interface and protein corona  
25  
26 complex, which play a pivotal role in the cellular uptake efficiency and biodistribution of the  
27  
28 nanomaterials throughout the body.  
29  
30  
31  
32  
33  
34  
35  
36  
37

38 Another aspect that needs to be addressed is the high-yield synthesis in order to contribute  
39  
40 with new affordable strategies compared to conventional methods, as well as the  
41  
42 improvement of their fluorescence QY with the aim to enhance their use as fluorescence  
43  
44 imaging agents.  
45  
46  
47  
48  
49

50 Undoubtedly, further exploration of biocompatible AuNC-based nanosystems must be  
51  
52 accompanied by theory–experiment investigations for driving this field forward and ideally,  
53  
54 to achieve their clinical translation in the near future.  
55  
56  
57  
58  
59  
60  
61  
62  
63  
64  
65



1  
2  
3  
4 **Acknowledgements**  
5  
6

7 This work was supported by the Academy of Finland (grants 294217, 292352, 319208 and  
8 HH's Academy Professorship).  
9  
10

11  
12  
13  
14  
15 **Conflict of Interest**  
16

17  
18  
19 The authors declare no conflict of interest.  
20  
21  
22  
23  
24

25 **References**  
26

- 27  
28 [1] S. E. Skrabalak, J. Chen, Y. Sun, X. Lu, L. Au, C. M. Cobley, Y. Xia, *Acc. Chem.*  
29 *Res.* **2008**, *41*, 1587.  
30  
31  
32  
33 [2] M. Homberger, U. Simon, *Philos. Trans. R. Soc. A Math. Phys. Eng. Sci.* **2010**, *368*,  
34 1405.  
35  
36  
37  
38 [3] P. Singh, S. Pandit, V. Mokkapati, A. Garg, V. Ravikumar, I. Mijakovic, *Int. J. Mol.*  
39 *Sci.* **2018**, *19*, 1979.  
40  
41  
42  
43 [4] Y.-C. Yeh, B. Creran, V. M. Rotello, *Nanoscale* **2012**, *4*, 1871.  
44  
45  
46  
47 [5] P. Chhour, P. C. Naha, R. Cheheltani, B. Benardo, S. Mian, D. P. Cormode, in  
48 *Nanomater. Pharmacol.*, Springer, **2016**, pp. 87–111.  
49  
50  
51  
52 [6] H. Daraee, A. Eatemadi, E. Abbasi, S. Fekri Aval, M. Kouhi, A. Akbarzadeh, *Artif.*  
53 *cells, nanomedicine, Biotechnol.* **2016**, *44*, 410.  
54  
55  
56  
57 [7] O. B. Adewale, H. Davids, L. Cairncross, S. Roux, *Int. J. Toxicol.* **2019**, *38*, 357.  
58  
59  
60  
61  
62  
63  
64  
65

- 1  
2  
3  
4 [8] C. M. Goodman, C. D. McCusker, T. Yilmaz, V. M. Rotello, *Bioconjug. Chem.*  
5  
6 **2004**, *15*, 897.  
7  
8  
9  
10 [9] Y. Pan, S. Neuss, A. Leifert, M. Fischler, F. Wen, U. Simon, G. Schmid, W.  
11  
12 Brandau, W. Jahnen- Dechent, *Small* **2007**, *3*, 1941.  
13  
14  
15 [10] J. F. Hainfeld, D. N. Slatkin, H. M. Smilowitz, *Phys. Med. Biol.* **2004**, *49*, N309.  
16  
17  
18 [11] R. Jin, C. Zeng, M. Zhou, Y. Chen, *Chem. Rev.* **2016**, *116*, 10346.  
19  
20  
21 [12] I. Chakraborty, T. Pradeep, *Chem. Rev.* **2017**, *117*, 8208.  
22  
23  
24 [13] H. Häkkinen, *From gold nanoparticles physics, Chem. Biol.* **2012**, *9*, 233.  
25  
26  
27 [14] T. Tsukuda, H. Häkkinen, *Protected Metal Clusters: From Fundamentals to*  
28  
29 *Applications*, Elsevier, **2015**.  
30  
31  
32  
33 [15] E. Porret, X. Le Guével, J.-L. Coll, *J. Mater. Chem. B* **2020**, *8*, 2216.  
34  
35  
36 [16] N. Kaur, R. N. Aditya, A. Singh, T.-R. Kuo, *Nanoscale Res. Lett.* **2018**, *13*, 302.  
37  
38  
39 [17] Z. Ma, P. Wang, L. Xiong, Y. Pei, *Wiley Interdiscip. Rev. Comput. Mol. Sci.* **2017**, *7*,  
40  
41 e1315.  
42  
43  
44 [18] H. Häkkinen, *Nat. Chem.* **2012**, *4*, 443.  
45  
46  
47 [19] S. Naahidi, M. Jafari, F. Edalat, K. Raymond, A. Khademhosseini, P. Chen, *J.*  
48  
49 *Control. release* **2013**, *166*, 182.  
50  
51  
52 [20] X.-D. Zhang, D. Wu, X. Shen, P.-X. Liu, F.-Y. Fan, S.-J. Fan, *Biomaterials* **2012**,  
53  
54 *33*, 4628.  
55  
56  
57 [21] C. N. Loynachan, A. P. Soleimany, J. S. Dudani, Y. Lin, A. Najer, A. Bekdemir, Q.  
58  
59  
60  
61  
62  
63  
64  
65

- 1  
2  
3  
4 Chen, S. N. Bhatia, M. M. Stevens, *Nat. Nanotechnol.* **2019**, *14*, 883.  
5  
6  
7 [22] A. K. Iyer, G. Khaled, J. Fang, H. Maeda, *Drug Discov. Today* **2006**, *11*, 812.  
8  
9  
10 [23] R. A. Petros, J. M. DeSimone, *Nat. Rev. Drug Discov.* **2010**, *9*, 615.  
11  
12  
13 [24] M. I. Setyawati, C. Y. Tay, B. H. Bay, D. T. Leong, *ACS Nano* **2017**, *11*, 5020.  
14  
15  
16 [25] K. L. D. M. Weerawardene, E. B. Guidez, C. M. Aikens, *J. Phys. Chem. C* **2017**,  
17  
18  
19  
20  
21  
22  
23 [26] H. Yu, B. Rao, W. Jiang, S. Yang, M. Zhu, *Coord. Chem. Rev.* **2019**, *378*, 595.  
24  
25  
26 [27] R. Mout, D. F. Moyano, S. Rana, V. M. Rotello, *Chem. Soc. Rev.* **2012**, *41*, 2539.  
27  
28  
29 [28] C. Auría-Soro, T. Nesma, P. Juanes-Velasco, A. Landeira-Viñuela, H. Fidalgo-  
30  
31  
32  
33  
34  
35  
36  
37  
38  
39  
40  
41  
42  
43  
44  
45  
46  
47  
48  
49  
50  
51  
52  
53  
54  
55  
56  
57  
58  
59  
60  
61  
62  
63  
64  
65
- [29] T.-T. Jia, G. Yang, S.-J. Mo, Z.-Y. Wang, B.-J. Li, W. Ma, Y.-X. Guo, X. Chen, X. Zhao, J.-Q. Liu, *ACS Nano* **2019**, *13*, 8320.
- [30] X. Zhang, Z. Luo, J. Chen, X. Shen, S. Song, Y. Sun, S. Fan, F. Fan, D. T. Leong, J. Xie, *Adv. Mater.* **2014**, *26*, 4565.
- [31] X. Zhang, J. Chen, Z. Luo, D. Wu, X. Shen, S. Song, Y. Sun, P. Liu, J. Zhao, S. Huo, *Adv. Healthc. Mater.* **2014**, *3*, 133.
- [32] X.-D. Zhang, Z. Luo, J. Chen, S. Song, X. Yuan, X. Shen, H. Wang, Y. Sun, K. Gao, L. Zhang, *Sci. Rep.* **2015**, *5*, 8669.
- [33] D. Luo, X. Wang, S. Zeng, G. Ramamurthy, C. Burda, J. P. Babilion, *Small* **2019**,

- 1  
2  
3  
4 15, 1900968.  
5  
6  
7 [34] Y. Yang, S. Wang, S. Chen, Y. Shen, M. Zhu, *Chem. Commun.* **2018**, 54, 9222.  
8  
9  
10 [35] L. Milane, M. Trivedi, A. Singh, M. Talekar, M. Amiji, *J. Control. release* **2015**,  
11 207, 40.  
12  
13  
14  
15 [36] E. Peterson, P. Kaur, *Front. Microbiol.* **2018**, 9, 2928.  
16  
17  
18 [37] P. V Baptista, M. P. McCusker, A. Carvalho, D. A. Ferreira, N. M. Mohan, M.  
19 Martins, A. R. Fernandes, *Front. Microbiol.* **2018**, 9, 1441.  
20  
21  
22  
23 [38] N.-Y. Lee, P.-R. Hsueh, W.-C. Ko, *Front. Pharmacol.* **2019**, 10, 1153.  
24  
25  
26 [39] K. Zheng, M. I. Setyawati, D. T. Leong, J. Xie, *ACS Nano* **2017**, 11, 6904.  
27  
28  
29 [40] B. Hammer, J. K. Norskov, *Nature* **1995**, 376, 238.  
30  
31  
32 [41] N. Lewinski, V. Colvin, R. Drezek, *small* **2008**, 4, 26.  
33  
34  
35 [42] J. Tang, H. Shi, G. Ma, L. Luo, Z. Tang, *Front. Bioeng. Biotechnol.* **2020**, 8, 1019.  
36  
37  
38 [43] L. P. Silva, A. P. Silveira, C. C. Bonatto, I. G. Reis, P. V Milreu, in *Nanostructures*  
39 *Antimicrob. Ther.*, Elsevier, **2017**, pp. 577–596.  
40  
41  
42 [44] V. Marjomäki, T. Lahtinen, M. Martikainen, J. Koivisto, S. Malola, K. Salorinne, M.  
43 Pettersson, H. Häkkinen, *Proc. Natl. Acad. Sci.* **2014**, 111, 1277.  
44  
45  
46 [45] M. Martikainen, K. Salorinne, T. Lahtinen, S. Malola, P. Permi, H. Häkkinen, V.  
47 Marjomäki, *Nanoscale* **2015**, 7, 17457.  
48  
49  
50 [46] Y. Yang, L. Wang, B. Wan, Y. Gu, *Front. Bioeng. Biotechnol.* **2019**, 7, 320.  
51  
52  
53 [47] M. Azubel, S. D. Carter, J. Weiszmann, J. Zhang, G. J. Jensen, Y. Li, R. D.  
54  
55  
56  
57  
58  
59  
60  
61  
62  
63  
64  
65

- 1  
2  
3  
4 Kornberg, *Elife* **2019**, *8*, e43146.  
5  
6  
7 [48] L. Shang, S. Dong, G. U. Nienhaus, *Nano Today* **2011**, *6*, 401.  
8  
9  
10 [49] H. Liu, G. Hong, Z. Luo, J. Chen, J. Chang, M. Gong, H. He, J. Yang, X. Yuan, L.  
11 Li, *Adv. Mater.* **2019**, *31*, 1901015.  
12  
13  
14  
15 [50] Y. Liu, J. Li, M. Chen, X. Chen, N. Zheng, *Theranostics* **2020**, *10*, 10057.  
16  
17  
18  
19 [51] L. Nie, M. Chen, X. Sun, P. Rong, N. Zheng, X. Chen, *Nanoscale* **2014**, *6*, 1271.  
20  
21  
22 [52] K. L. D. M. Weerawardene, H. Häkkinen, C. M. Aikens, *Annu. Rev. Phys. Chem.*  
23 **2018**, *69*.  
24  
25  
26  
27 [53] S. Malola, H. Häkkinen, *J. Am. Chem. Soc.* **2019**, *141*, 6006.  
28  
29  
30  
31 [54] M. F. Matus, S. Malola, E. K. Bonilla, B. Barngrover, C. M. Aikens, H. Häkkinen,  
32 *Chem. Commun.* **2020**, *56*, 8087.  
33  
34  
35  
36 [55] E. Pohjolainen, X. Chen, S. Malola, G. Groenhof, H. Häkkinen, *J. Chem. Theory*  
37 *Comput.* **2016**, *12*, 1342.  
38  
39  
40  
41  
42 [56] M. J. Hostetler, A. C. Templeton, R. W. Murray, *Langmuir* **1999**, *15*, 3782.  
43  
44  
45 [57] R. Guo, Y. Song, G. Wang, R. W. Murray, *J. Am. Chem. Soc.* **2005**, *127*, 2752.  
46  
47  
48 [58] M. Montalti, L. Prodi, N. Zaccheroni, R. Baxter, G. Teobaldi, F. Zerbetto, *Langmuir*  
49 **2003**, *19*, 5172.  
50  
51  
52  
53 [59] C. L. Heinecke, T. W. Ni, S. Malola, V. Mäkinen, O. A. Wong, H. Häkkinen, C. J.  
54 Ackerson, *J. Am. Chem. Soc.* **2012**, *134*, 13316.  
55  
56  
57  
58  
59 [60] V. Rojas-Cervellera, L. Raich, J. Akola, C. Rovira, *Nanoscale* **2017**, *9*, 3121.  
60  
61  
62  
63  
64  
65

- 1  
2  
3  
4 [61] C. J. Ackerson, P. D. Jadzinsky, G. J. Jensen, R. D. Kornberg, *J. Am. Chem. Soc.*  
5  
6 **2006**, *128*, 2635.  
7  
8  
9  
10 [62] K. Salorinne, S. Malola, O. A. Wong, C. D. Rithner, X. Chen, C. J. Ackerson, H.  
11  
12 Häkkinen, *Nat. Commun.* **2016**, *7*, 1.  
13  
14  
15 [63] P. D. Jadzinsky, G. Calero, C. J. Ackerson, D. A. Bushnell, R. D. Kornberg, *Science*  
16  
17 (*80-*). **2007**, *318*, 430.  
18  
19  
20  
21 [64] T.-R. Tero, S. Malola, B. Koncz, E. Pohjolainen, S. Lautala, S. Mustalahti, P. Permi,  
22  
23 G. Groenhof, M. Pettersson, H. Häkkinen, *ACS Nano* **2017**, *11*, 11872.  
24  
25  
26 [65] M. Azubel, R. D. Kornberg, *Nano Lett.* **2016**, *16*, 3348.  
27  
28  
29  
30 [66] M. Azubel, A. L. Koh, K. Koyasu, T. Tsukuda, R. D. Kornberg, *ACS Nano* **2017**, *11*,  
31  
32 11866.  
33  
34  
35 [67] E. Pohjolainen, S. Malola, G. Groenhof, H. Häkkinen, *Bioconjug. Chem.* **2017**, *28*,  
36  
37 2327.  
38  
39  
40  
41  
42  
43  
44  
45  
46  
47  
48  
49  
50  
51  
52  
53  
54  
55  
56  
57  
58  
59  
60  
61  
62  
63  
64  
65

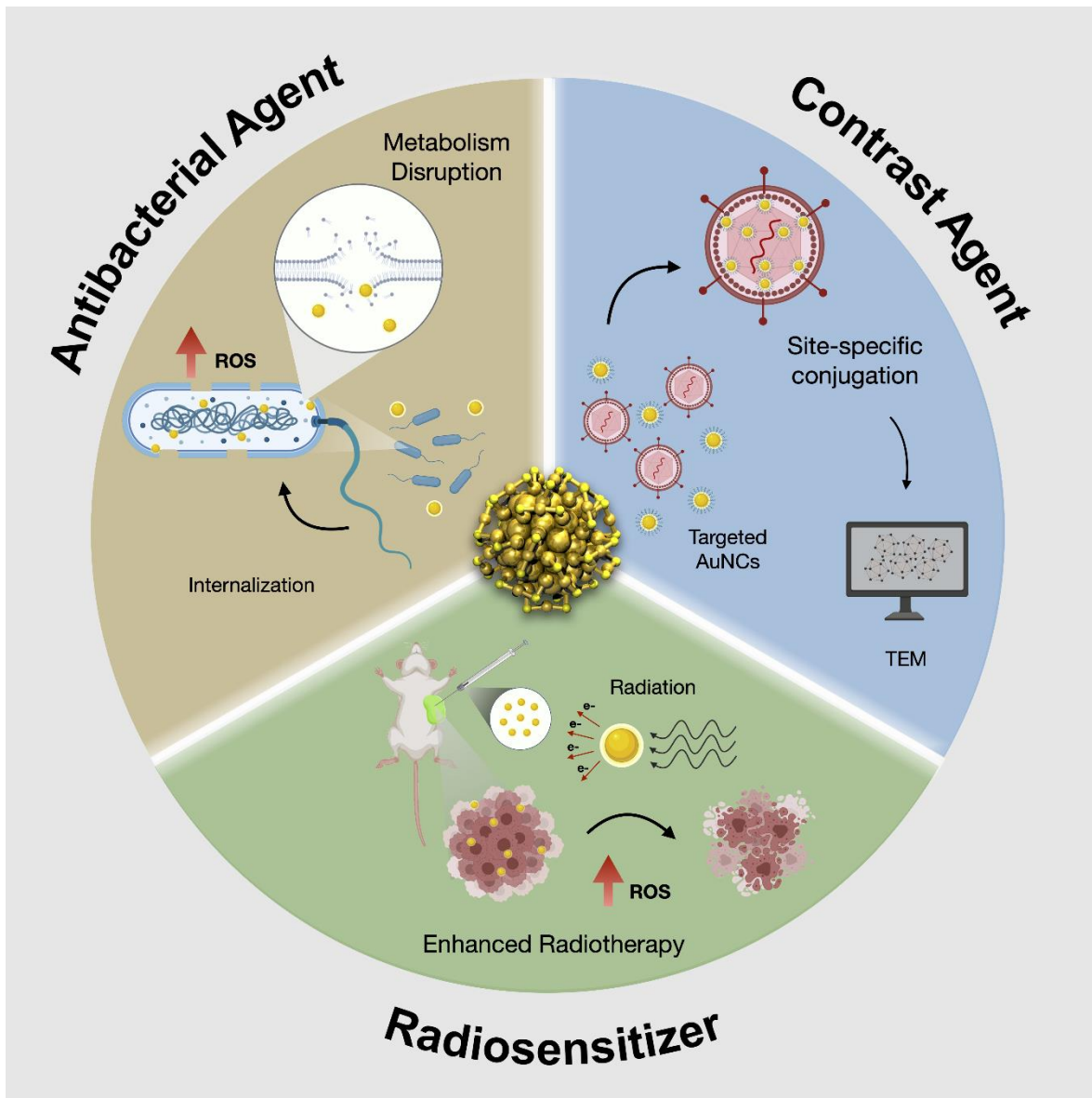


**Figure 1.** Representative examples of biomedical applications reported by atomically-precise AuNCs: Antimicrobial applications, biological imaging, and radiation therapy. ROS: Reactive Oxygen Species; TEM: Transmission Electron Microscopy.

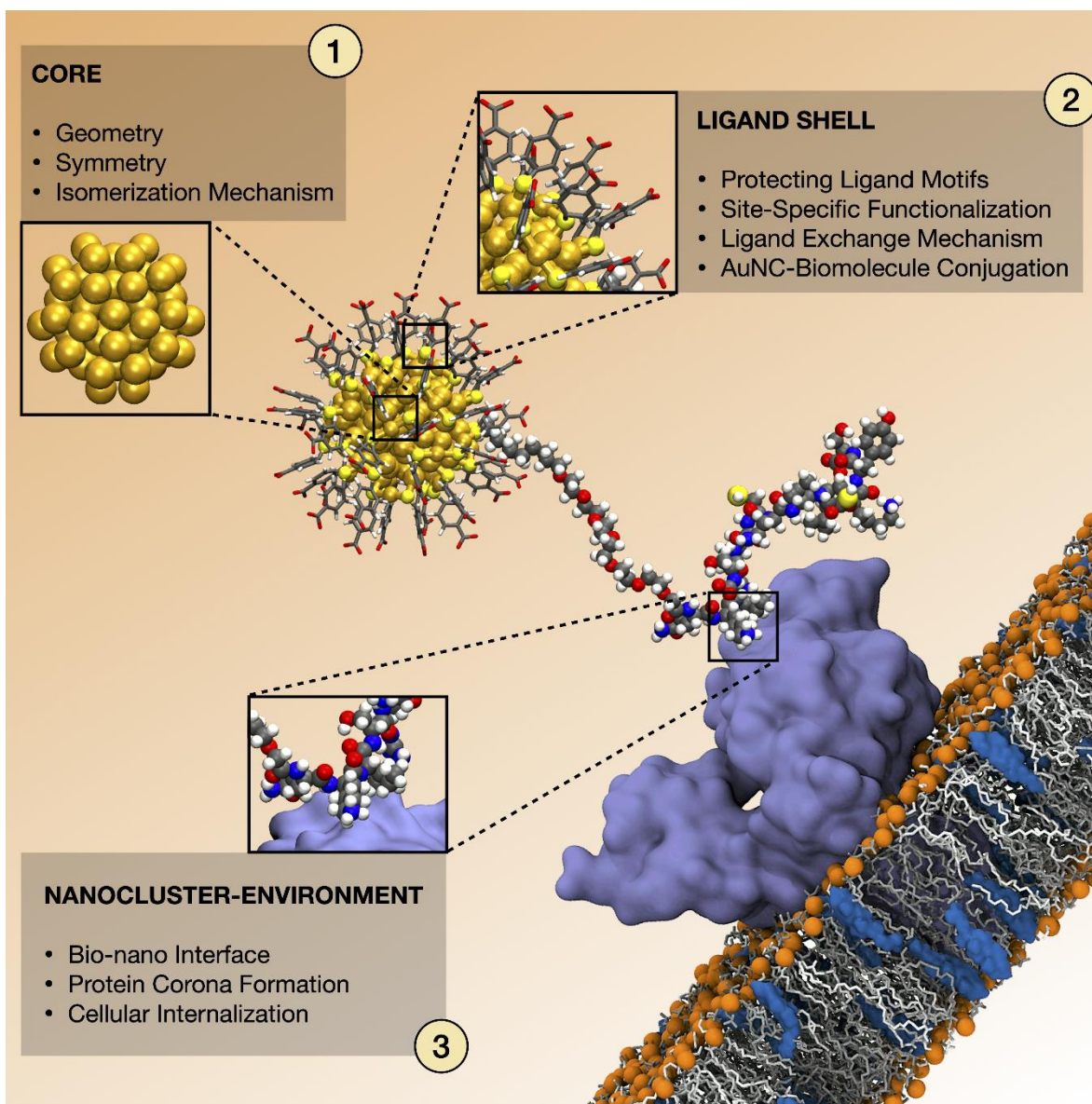
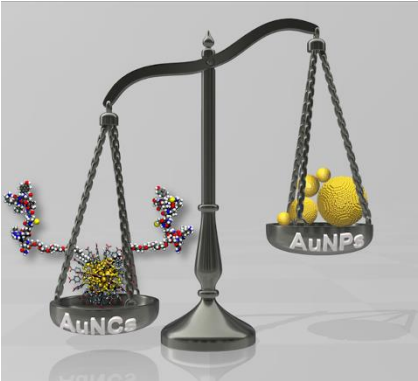


**Figure 2.** Schematic illustration showing the main aspects that can be precisely explored in the design of biocompatible gold nanoclusters (AuNCs)-based systems by employing a theoretical–experimental approach. A partially exchanged  $\text{Au}_{102}(\text{pMBA})_{43}(\text{peptide})_1$  nanocluster is depicted near a typical bilayer of phospholipids. Different physicochemical properties of AuNCs can be either predicted or revealed by a combination of theory (quantum mechanics or molecular mechanics methods) and experimental studies at three levels: 1) core, 2) ligand shell, and 3) nanocluster-environment interface.



1  
2  
3  
4  
5  
6  
7  
8  
9  
10  
11  
12  
13  
14  
15  
16  
17  
18  
19  
20  
21  
22  
23  
24  
25  
26  
27  
28  
29  
30  
31  
32  
33  
34  
35  
36  
37  
38  
39  
40  
41  
42  
43  
44  
45  
46  
47  
48  
49  
50  
51  
52  
53  
54  
55  
56  
57  
58  
59  
60  
61  
62  
63  
64  
65

ToC Figure



Atomically precise gold nanoclusters (AuNCs) have helped revolutionize nanomedicine's field due to their excellent biocompatibility and extraordinary physicochemical properties. They have emerged as promising materials to overcome the current challenges of cytotoxicity and biostability present in colloidal gold nanoparticles. Although this revolution is still in its infancy, theoretical/experimental strategies show that the near future is promising!



18  
19  
20  
21  
22  
23  
24  
25  
26  
27  
28  
29  
30  
31  
32  
33  
34  
35  
36  
37  
38

**Dr. María Francisca Matus** is a Postdoctoral Researcher in the Nanoscience Center (NSC) at the University of Jyväskylä (Finland) under the direction of Prof. Dr. Hannu Häkkinen. She received her Ph.D. in Science in 2018 at the University of Talca (Chile), where her work was focused on the study and characterization of polymeric nanoparticles as drug delivery systems for cardiovascular diseases. Her recent research focuses on the design and development of multifunctional gold nanoclusters for targeted cancer therapy through theoretical/experimental strategies.



52  
53  
54  
55  
56  
57  
58  
59  
60  
61  
62  
63  
64  
65

**Prof. Dr. Hannu Häkkinen** is a professor in computational nanoscience at the University of Jyväskylä in Finland and a visiting professor in Xiamen, China. His research interests include electronic, optical, magnetic, chemical and catalytic properties of bare, supported, and ligand-protected metal nanoparticles, electrical conductivity of molecule-metal interfaces in

1  
2  
3  
4  
5  
6  
7  
8  
9  
10  
11  
12  
13  
14  
15  
16  
17  
18  
19  
20  
21  
22  
23  
24  
25  
26  
27  
28  
29  
30  
31  
32  
33  
34  
35  
36  
37  
38  
39  
40  
41  
42  
43  
44  
45  
46  
47  
48  
49  
50  
51  
52  
53  
54  
55  
56  
57  
58  
59  
60  
61  
62  
63  
64  
65

nanostructures, and structural and chemical properties of metal nanoparticle / virus hybrids.  
He has been working on modeling gold nanoclusters for 20 years. He has published about  
250 peer-reviewed articles with over 21000 citations and his h-index is 68 (Web of Science).  
In 2018, he was listed as one of the “Highly Cited Researchers” by Clarivate Analytics.